

# Apparent Slip of Newtonian Fluids Past Adsorbed Polymer Layers

Yingxi Zhu and Steve Granick\*

Department of Materials Science and Engineering, University of Illinois, Urbana, Illinois 61801

Received January 10, 2002

**ABSTRACT:** We show unexpected drag reduction as solvent flows past polymer-coated surfaces in solution. Adsorbed polymer layers of two types, poly(vinyl alcohol) (PVA) homopolymers in deionized water and poly(vinylpyridine)–polybutadiene diblock copolymers (PVP–PB) in tetradecane, were placed at variable spacings larger than twice the layer thickness within a modified surface forces apparatus, and the hydrodynamic forces owing to flow of solvent past these layers were measured as a function of surface spacing, pumping frequency, and pumping velocity (product of frequency and amplitude). When the flow rate was below a critical level, which depended on the system, the findings agreed with a simple hydrodynamic picture in which the solvent appeared to flow past surfaces of defined spacing, the solid–solid spacing less than twice the “hydrodynamic radius” ( $R_H$ ). The value of  $R_H$  was not always constant, however. In the PVA system it tripled as frequency was raised from 1 to 50 Hz though it was frequency-independent in the PVP–PB system. There was also strong dependence on flow rate. When the flow rate exceeded a critical level, the magnitude of hydrodynamic forces became up to an order of magnitude less than can be described by flow past a layer of thickness  $R_H$  and the “stick” boundary condition at that layer. A striking observation, which we present without definitive explanation at this time, is that when the flow rates were sufficiently high, the hydrodynamic forces decreased below those for flow of these solvents with no polymer layer at the surface and the “stick” boundary condition. The onset of this drag reduction occurred at the peak shear stress of 8 pN molecule<sup>−1</sup> (PVP–PB) or 12 pN molecule<sup>−1</sup> (PVA).

## Introduction

“Hairy” surfaces—polymer chains tethered to surfaces in a liquid environment—present complex physical problems decidedly different from hard, rigid surfaces, owing to the diffuse nature of the polymer layers. We are interested here in their response to flow of solvent past them. The present study focuses upon the influence of the surface texture on the flow of a Newtonian liquid external flow past it. Flow-induced deformations of polymer conformations at the surface are also of parallel interest.<sup>1–5</sup> Both of these issues contrast with those of equilibrium surface–surface interactions, which have seen much attention and are now well understood.<sup>6,7</sup> Furthermore, this problem has significant practical relevance because the magnitude of hydrodynamic forces between surfaces in relative motion may easily exceed the equilibrium forces.<sup>8,9</sup> Incomplete understanding of these issues has implications in numerous areas where hairy surfaces are exposed to fluid flow—from tribology to biology, as for example to the flow of blood—and to the hydrodynamic interactions of sterically stabilized colloidal particles.

In particular, we inquire here into the far-field situation where the polymer-laden surfaces are far enough apart to be separated by pure solvent. Recent experimental<sup>10–13</sup> and simulation studies<sup>14–17</sup> show that Newtonian fluids appear to “slip” when they flow past rigid molecularly smooth surfaces, provided that the flow rate exceeds a system-specific necessary level.<sup>11,13,14</sup> But “stick” is expected to be recovered if the solid surfaces are sufficiently rough,<sup>18–20</sup> so it becomes interesting to introduce small amounts of roughness deliberately. Elsewhere, we describe a study of the effects of topographical roughness.<sup>21</sup> Here surface roughness of a different type, a diffuse surface layer, is introduced by the mechanism of allowing soluble polymer chains to adsorb from solution.

There is a standard textbook interpretation: the polymer layer renormalizes the location of the solid surface to a new location, the actual solid surface plus the “hydrodynamic radius” of surface-tethered polymer, and fluid on the surface of the renormalized moving body moves at the same rate as that body.<sup>22–24</sup> (Another limiting case, the near-field situation, occurs if the polymer-laden surfaces are so close together that the chain conformations overlap. Then the flow of solvent through these chains is perhaps akin to the flow of solvent through a porous medium,<sup>25,26</sup> albeit one whose structure adjusts to flow.<sup>1–5,27,28</sup>) Here, in studying the far-field situation, we show that this picture appears to break down when the flow rate (and therefore the shear stress on the chains at the moving surface) exceeds a critical level. The surprising result emerges that viscous dissipation of these Newtonian liquid solvents actually becomes less than for their flow past rigid surfaces in the absence of adsorbed polymer.

Two systems were studied. We began with statistically adsorbed poly(vinyl alcohol) homopolymer in water but, in the face of the surprising results described below, then performed control experiments in a simpler model system, diblock copolymer brushes in a nonpolar solvent, selected because its equilibrium properties have been studied exhaustively,<sup>6</sup> and this laboratory has previous experience with it.<sup>27</sup> Despite quantitative differences between these systems, the main qualitative conclusions were the same.

## Experimental Section

To measure hydrodynamic forces over a wide range of velocity, but at given surface–surface separations, we employed methods of piezoelectric actuation in a modified surface forces apparatus described elsewhere.<sup>13,27,28</sup> Multiple beam interferometry between silver sheets on the backside of cleaved single crystals of mica was used to measure the surface separation. After placing surfaces at a given spacing, they were

pumped in the normal direction with small-amplitude oscillatory modulations of spacing, so that the peak velocity varied while keeping the spacing nearly constant. More specifically, the amplitudes and frequencies of modulation were controlled independently, thus allowing the mean velocity to vary over a large range without concomitant large change of the spacing itself. The data presented below were obtained using a lock-in amplifier, but full inspection of the shape of the response functions using an oscilloscope showed them to be linear. The film thicknesses were measured with a resolution of 5 Å using optical interferometry, and the dynamic forces were measured with a resolution of  $10^{-7}$  N using piezoelectric methods. The geometry was cylindrically shaped surfaces, with radius of curvature  $R \approx 2$  cm, that were oriented at right angles to one another. The separations reported below refer to separations between the single-crystal muscovite mica between which the polymers and solvent were later deposited. We analyze here the viscous response,  $90^\circ$  out of phase with the sinusoidal drive. The signal at  $0^\circ$  phase shift can be used to determine the conservative forces, as we have done elsewhere.

The diblock copolymers of polybutadiene and poly(vinylpyridine) (PB–PVP), donated by Prof. H. Watanabe of the Institute of Chemical Research at Kyoto University, possessed molecular weight 38 500 (PB) and 23 700 (PVP). The ratio weight-average to number-average molecular weight was  $M_w/M_n < 1.05$ . Freshly cleaved mica strips glued onto cylindrical disks were first calibrated in the SFA to determine the mica thickness and then immersed into 5  $\mu\text{g/mL}$  PB–PVP toluene (Aldrich) solution for 2 h, whose concentration was far below the critical micelle concentration. Because toluene was a good solvent for PB but a nonsolvent for PVP, the PVP block selectively adsorbed onto the mica substrate with the PB block standing up. After adsorption, surfaces were rinsed with toluene for achieving absence of nonadsorbed polymer chains and purged of toluene with argon gas. Finally, the dried polymer-coated surfaces were mounted into the SFA and filled with a droplet of tetradecane in between. For experiments with the PVA-coated system, 0.1 mg/mL PVA (Aldrich, 87–89% hydrolyzed,  $M_n = 12\,300$ – $18\,600$ ) aqueous solution was prepared by stirring for 3–4 h deionized water previously heated to  $80^\circ\text{C}$ .

The thickness of dried polymer layers was measured after experiments in order to estimate surface coverage. The dry PB–PVP layer thickness was 32 Å, which amounted to the grafting density of  $2.3 \times 10^{16}$  chains  $\text{m}^{-2}$ , or an average spacing between anchor points of 6.5 nm,<sup>15</sup> calculated from the known density. And for the dried PVA layer the thickness was 1.6 nm, corresponding to about  $7.8 \times 10^{18}$  chains  $\text{m}^{-2}$ , i.e.,  $\sim 0.8$  mg  $\text{m}^{-2}$ .

## Results and Discussion

Dynamic oscillatory changes of spacing between curved surfaces create a pressure gradient that drives fluid out of (and into) this gap. Motion is opposed by the viscous drag of solvent. For Newtonian fluids and rigid surfaces the hydrodynamic force  $F_H$  is proportional to the fluid viscosity,  $\eta$ , and to the rate at which spacing changes,  $dD/dt$  ( $D$  denotes spacing and  $t$  denotes time), and diverges as  $1/D$ . The resulting expression is a generalization of Stokes' law of viscous flow:

$$F_H = \frac{6\pi R^2 \eta}{D} \frac{dD}{dt} \quad (1)$$

where  $R$  is the mean radius of curvature of the two cylindrical surfaces. High-order solutions of the Navier–Stokes equations essentially confirm this expression, known as the Reynolds equation.<sup>23</sup> When the surface spacing is vibrated, the prediction is analogous if  $dD/dt$  is identified with the peak velocity of vibration,  $v_{\text{peak}} = d\omega$ , where  $d$  is vibration amplitude and  $\omega$  the radian frequency of vibration.<sup>29</sup> Experimental tests with thin

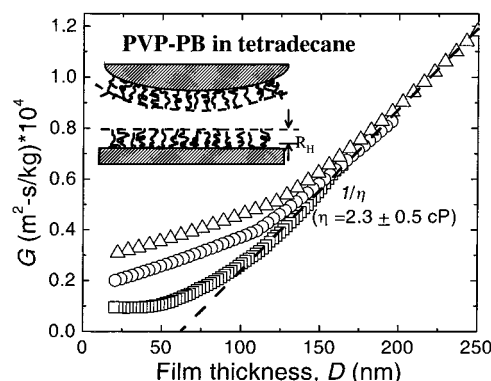


**Figure 1.** For the end-attached PB chains (adsorbed PVP–PB diblock copolymers), the reciprocal of hydrodynamic forces ( $G = 6\pi R^2 v_{\text{peak}}/F_{H,\text{peak}} = (D - 2R_H)/\eta$ , of order  $10^{-4}$   $\text{m}^2 \text{s/kg}$ ) for PB undergoing 2.6 Hz oscillation at variable amplitude, 0.6 nm (squares), 1 nm (circles), 2 nm (triangles). The reciprocal of the slope at large film thickness yielded the known viscosity of the flowing solvent, tetradecane,  $\eta = 2.3 \pm 0.5$  cP at  $25^\circ\text{C}$ . The intercept gave twice  $R_H$ , the hydrodynamic layer thickness of an adsorbed or grafted polymer. Inset: cartoon of the experimental configuration.

films of nonpolar, Newtonian fluids confined between mica surfaces agree with this prediction down to a spacing of 2–5 molecular dimensions ( $< 1$  nm),<sup>13,30–32</sup> confirming the quantitative validity of this continuum description if the surfaces are fully wetted by the solvent.

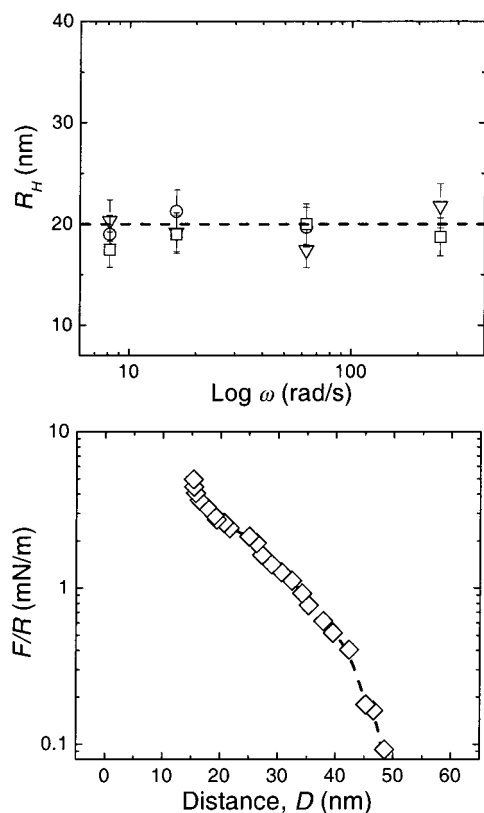
As already noted, dynamic interactions of polymer-coated “hairy” surfaces separated by solvent have often been believed to obey the same expression provided that  $D$  is replaced by  $D' \equiv D - 2R_H$ , where  $R_H$  is the “hydrodynamic thickness” of the hairy carpet on each surface.<sup>7,33,34,35</sup>

$$F_H = \frac{6\pi R^2 \eta}{D - 2R_H} \frac{dD}{dt} \quad (2)$$

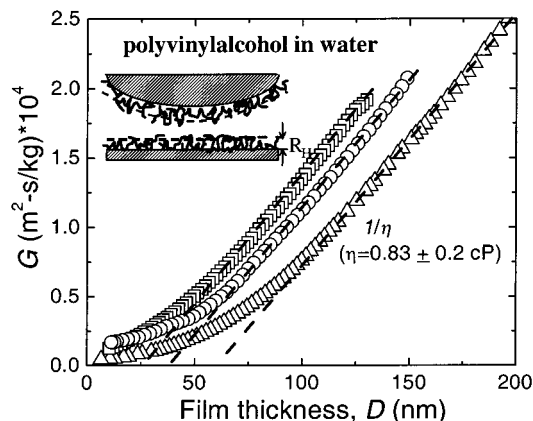
### End-Tethered Polymers in a Nonpolar Solvent.

Figure 1 shows raw data for the PVP–PB system in tetradecane solvent. In the limit of slower flow rates than emphasized here, this laboratory previously studied hydrodynamic flow in this same system.<sup>27</sup> These data in this figure are compared with a linearization of eq 1, and the quantity  $G = 6\pi R^2 v_{\text{peak}}/F_{H,\text{peak}} = (D - 2R_H)/\eta$  is plotted against surface spacing. One sees that at the largest surface spacings the data fell on a straight line whose inverse slope equals the known viscosity of water. The extrapolation to zero on the ordinate established the hydrodynamic thickness of two opposed polymer layers,  $2R_H$ , thus determining the effective surface–surface spacing,  $D' \equiv D - 2R_H$ , in the classical fashion. From prior work it was already known that data approaching this point become curved; the data exceeded the linear extrapolation from larger separation.<sup>26,29,33</sup> The novel finding presented here is that these deviations were larger, and set in at larger thickness, the more rapid the flow rate.

The bottom panel of Figure 2 shows the static force–distance profile; it is monotonically repulsive and has been analyzed elsewhere.<sup>27</sup> The equilibrated forces that resisted compression, normalized by the mean radius of curvature, are plotted against separation on semi-logarithmic scales. The top panel plots the hydrodynamic radius against logarithmic frequency. One observes that it was approximately half the film thick-



**Figure 2.** Top panel: hydrodynamic thickness plotted vs logarithmic pumping frequency for data of the type illustrated in Figure 1. The data were compared at variable applied amplitude, 0.6 nm (squares), 1 nm (circles), 2 nm (triangles). Bottom panel: static force–distance profile.



**Figure 3.** Reciprocal of hydrodynamic forces ( $G$ , of order  $10^{-4}$   $\text{m}^2 \text{s/kg}$ ) for poly(vinyl alcohol) (PVA) at 1.0 nm amplitude oscillation at variable frequency, 2.6 Hz (squares), 10 Hz (circles), 40 Hz (triangles). The reciprocal of the slope at large film thickness yielded the known viscosity of the flowing solvent, water,  $\eta = 0.83 \pm 0.2$  cP at 25 °C. The intercept gave twice  $R_H$ , the hydrodynamic layer thickness of an adsorbed or grafted polymer.

ness at onset of static forces. In contrast to the PVA system discussed next,  $R_H$  did not depend on oscillatory frequency.

**Statistically Adsorbed Polymer in Aqueous Solution.** The aqueous PVA system is widely used to stabilize colloidal particles against aggregation during processing.<sup>36</sup> Figure 3 shows selected raw data,  $G$  plotted against  $D$  in the manner described above. One observes that while data taken at a given frequency could be extrapolated to zero to define hydrodynamic

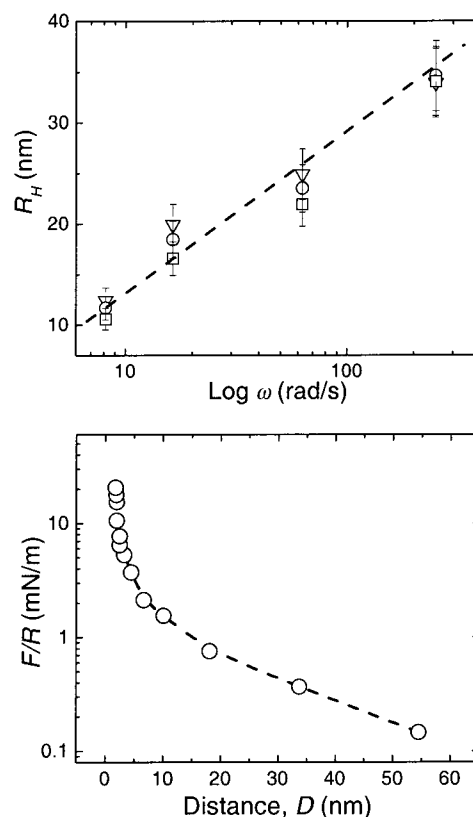


**Figure 4.** Top panel: hydrodynamic thickness ( $R_H$ ) plotted vs logarithmic frequency for adsorbed PVA chains in deionized water. The data were compared at variable applied amplitude, 0.6 nm (squares), 1 nm (circles), 2 nm (triangles). Bottom panel: static force–distance profile.

thickness  $R_H$ , in this system  $R_H$  grew with increasing frequency. But just as for the PVP–PB system, deviations from linearity were larger, and set in at larger thickness, the larger the oscillation amplitude.

The bottom panel of Figure 4 shows the static force–distance profile, which was monotonically repulsive. As the adsorption of PVA onto mica surface is driven by hydrogen bonding, PVA layers exhibited a more compressible structure than end-grafted PB, indicated by smaller “hard-wall” thickness. The top panel of Figure 4 plots  $R_H$  against logarithmic frequency. The frequency dependence in this system contrasts with the PVP–PB system, and probably signifies that the dynamical responses in these layers are slower, within the range spanned by the inverse applied frequency. Therefore, the more rapid the experiment (the higher the frequency), the larger the hydrodynamic thickness. This difference between systems is in a reasonable direction; it makes sense physically that response times are slower for an adsorbed rather than end-tethered polymer layer, because an end-tethered layer has many fewer modes of possible viscoelastic response. Frequency dependence was also observed years ago by Israelachvili and co-workers in a melt of polybutadiene oligomers.<sup>37</sup> This effect, observed now independently in a different laboratory, seems to be general.

**Apparent Slip.** Now we discuss more carefully the regime where our observations failed to fit eq 2, but  $D > 2R_H$ . For quantification, we computed the ratio

$$f^* = \frac{F_H(\text{observed})}{F_H(\text{from eq 2})} \quad (3)$$

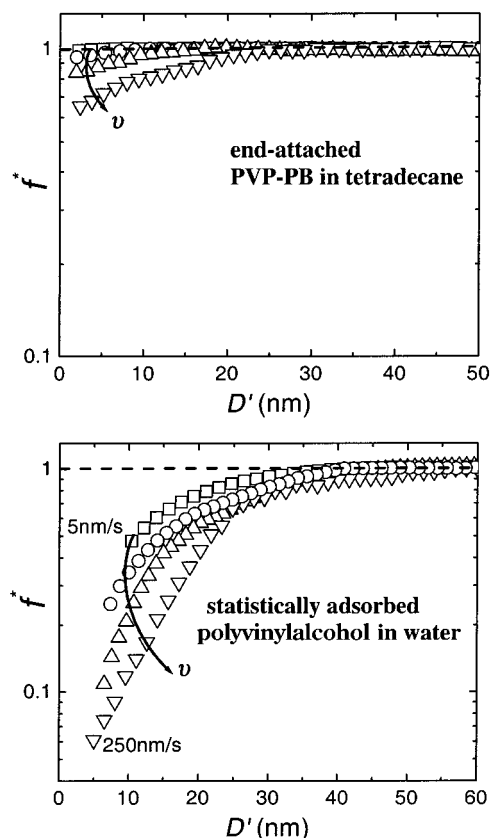


**Figure 5.** Dimensionless parameter  $f^*$ , the ratio of actual hydrodynamic force to that predicted from eq 2, plotted against layer spacing, for flow of Newtonian solvents past two polymer systems. The  $f^*$  parameters are plotted on log-log scales against the layer spacing ( $D' = D - 2R_H$ ) at variable peak velocity. Top panel shows the influence of velocity of solvent flow for end-attached layers of PVP-PB in tetradecane. Bottom panel shows the influence of solvent flow for PVA in deionized water. For both two systems, the peak velocity of vibration,  $v_{\text{peak}} = d\omega$ , was 5 nm s<sup>-1</sup> (squares), 40 nm s<sup>-1</sup> (circles), 125 nm s<sup>-1</sup> (up triangles), and 250 nm s<sup>-1</sup> (down triangles). The arrow shows the direction of increasing velocity.

i.e., the ratio of the actual hydrodynamic force to the level predicted from eq 2. Figure 5 (top panel) plots  $\log f^*$  against  $D'$  for the PVP-PB system; Figure 5 (bottom panel) plots the same thing for the PVA system. Both collections of data are plotted for instances in which the surface spacing was vibrated dynamically with different peak velocity. In both panels, one observes that  $f^*$  decreased more and more below unity, the more rapidly that the surface spacing was varied. For example, at  $D = 8$  nm (bottom panel), the hydrodynamic force was 10 times less than predicted by eq 2. Curvature in empirical data of this sort has been reported previously by several research groups including this one<sup>26-29,34,37</sup> but without, to the best of our knowledge, this quantitative analysis of its implications.

Independent of subsequent analysis, it is worth emphasizing the extreme fluidity that is summarized in these data. In Figure 1, for example, solvent in the absence of polymer would show the same slope but would intercept the origin.<sup>23</sup> But some of the data in Figure 1 lie above this notional line. In other words, in the presence of polymer, and at high enough flow rates, the resistance to flow was less than if no polymer had been present.

Seeking explanation, one might argue that the viscosity term in eq 2 underwent shear thinning, but this

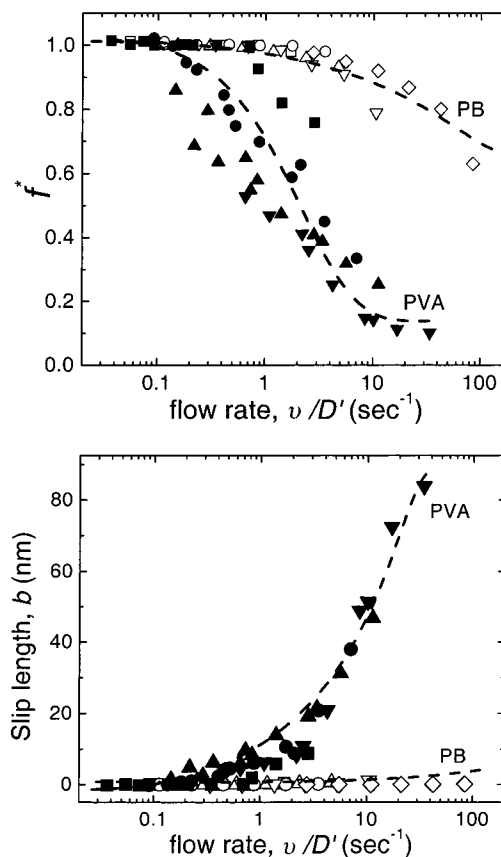


**Figure 6.** Top panel: the parameter  $f^*$  (the ratio of actual hydrodynamic force to that predicted from eq 2) is plotted on log-log scales against logarithmic reduced flow rate,  $v_{\text{peak}}/D'$ . Bottom panel: slip length, calculated from eq 4. The data concern deionized water between adsorbed layers of PVA (solid symbols) and tetradecane between end-grafted PB brushes (open symbols). Reduced flow rate is the peak velocity of liquid, responding to the peak velocity of vibration varying from 5 to 250 nm s<sup>-1</sup>, normalized by the layer spacing,  $D' = D - 2R_H$ . For both two systems, the data refer to film thickness of 50 nm (squares), 24 nm (circles), 18 nm (upper triangles), 8 nm (down triangles), and 2 nm (diamonds).

argument is unphysical because the solvent was a low-viscosity Newtonian fluid. One might argue that the velocity field of solvent flow penetrated into the adsorbed polymer layers, into the regime of thickness where  $D < 2R_H$  (as has been considered theoretically<sup>25</sup>), but this line of argument, which is certainly plausible, cannot explain why fluidity exceeded what would be anticipated for a Newtonian fluid if no polymer were present at all. One is driven to consider the possibility that the presence of polymer somehow altered the coupling of momentum transfer between the surface and the moving fluid.

Further investigation showed empirically that  $f^*$  did not scale with either velocity or surface spacing considered separately, but with their ratio. The same empirical scaling was suggested from considering the flow of Newtonian fluids past rigid surfaces.<sup>13</sup> This quantity,  $v_{\text{peak}}/D'$ , we identify with the flow rate.

In Figure 6 (top panel),  $f^*$  is plotted against logarithmic flow rate for both systems; the flow rate varied by more than 3 orders of magnitude. There is scatter, but less than appears, if one considers the large changes in the variables, especially the peak velocity. The pattern in both systems was qualitatively the same: agreement with eq 2 until the flow rate exceeded a

critical level, followed by deviations in the direction of more fluidity than expected.

Alternatively, there is a tradition in fluid dynamics to infer the "slip length", the fictive distance inside the solid at which the no-slip flow boundary condition would hold. Without necessarily assigning physical meaning to this quantity, it can be used as an alternative expression of the same data. Mathematical manipulation<sup>38</sup> shows that  $f^*$  and slip length ( $b$ ) are related as

$$f^* = 2 \frac{D}{6b} \left[ \left( 1 + \frac{D}{6b} \right) \ln \left( 1 + \frac{6b}{D} \right) - 1 \right] \quad (4)$$

This expression of the data is also plotted in Figure 6 (bottom panel).

In the "stick" regime ( $f^* = 1$ ), where the flow rate was sufficiently slow that eq 2 was obeyed, it is appropriate to invoke the known formalisms that allows one to calculate shear rate and shear stress of the moving fluid on the solid body. These quantities, the maximum shear rate and the maximum shear stress, on the coincident apex of the crossed cylinders, were calculated using the equations derived by Vinogradova.<sup>38</sup> This analysis shows that no deviations from eq 2 were observed up to  $1.8 \times 10^5$  Pa peak stress (PVP-PB) and  $9.6 \times 10^4$  Pa peak stress (PVA), which are equivalent to the peak shear rates of  $7 \times 10^3$  and  $1.15 \times 10^3$  s<sup>-1</sup>, respectively. Shear rate is often considered to be the controlling variable in rheology literature, but shear stress is considered when considering slip of high-viscosity polymer melts. This is why we report both. In any event, the main point is that fluidity increased only when these critical levels were exceeded. In addition, the mean area per molecule was known from the amount adsorbed, so the critical shear stress was equivalent to 8 pN molecule<sup>-1</sup> (PVP-PB) or 12 pN molecule<sup>-1</sup> (PVA).

## Outlook

We present this study as empirical observation that lacks definitive explanation. Perhaps the main point is the large deviations observed from eq 2, which has been widely used approximation for analyzing the flow of solvent past adsorbed polymer layers.

Clearly, a complete analysis of this problem would consider the penetration of solvent velocity field into the adsorbed polymer structure, and the data appear to indicate that this velocity field may change according to flow rate (though this statement is speculative). But it is not clear presently why, at high enough flow rates, the resistance to flow was less than if no polymer had been present at all. In fact, with increasing shear it has been predicted that polymer layers will expand<sup>4</sup> or contract<sup>5</sup>—there appears to be yet no definitive physical understanding of this point.

Although explanation remains unclear, in seeking to explain the occurrence of slip there is a tempting analogy to make with the flow of oil droplets in water. The polymer layers in these experiments were predominantly comprised of solvent; the mean solvent content in the large volume that they pervaded was  $\approx 99\%$ . In another area of study, it is known that fluid droplets immersed in an immiscible fluid<sup>23</sup> and also fluid-encapsulated solid particles<sup>39</sup> sustain weaker hydrodynamic forces than rigid spheres because the fluid within the droplets also participates in the flow. In this scenario, the polymer chains on our solids may have

functioned as a sort of fluid membrane that encapsulated them. The analogy is imperfect because these layers were surface-attached, so that flow of solvent within them cannot obey the continuum fluid mechanical equations that have been supposed in those fields of study, but we speculate tentatively that the physical idea may carry over.

From the practical standpoint, this has evident bearing on understanding a variety of physical situations where fluid flows past polymer-laden surfaces at rapid rate—especially filtration and the flow and the dispersion and aggregation of colloidal particles such as foods, paints, and other disperse phases. There is also possible relevance to controlling water flow past ships and fish,<sup>40</sup> microfluidic devices,<sup>41</sup> and fluid flow in biological organs such as the kidney.<sup>42</sup>

**Acknowledgment.** We are grateful to Jack F. Douglas for discussions. This work was supported primarily by the U.S. Department of Energy, Division of Materials Science, under Award DEFG02-91ER45439 to the Frederick Seitz Materials Research Laboratory at the University of Illinois at Urbana-Champaign, and in part by the National Science Foundation (Tribology Program).

## References and Notes

- Brochard, F.; Buguin, A. C. *R. Acad. Sci. II B* **1995**, *321*, 463.
- Baker, S. M.; Smith, G. S.; Anastassopoulos, D. L.; Toprakcioglu, C.; Vradis, A. A.; Bucknall, D. G. *Macromolecules* **2000**, *33*, 1120.
- Soga, I.; Granick, S. *Langmuir* **1998**, *14*, 4266.
- Doyle, P. S.; Shaqfeh, E. S. G.; Gast, A. P. *Macromolecules* **1998**, *31*, 5474.
- For a review, see: Grest, G. S. *Adv. Polym. Sci.* **1999**, *138*, 149.
- Halperin, A.; Tirrell, M. V.; Lodge, T. P. *Adv. Polym. Sci.* **1992**, *100*, 31.
- Fleer, G. J.; Cohen Stuart, M. A.; Scheutjens, J. M. H. M.; Cosgrove, T.; Vincent, B. *Polymers at Interfaces*; Chapman and Hall: New York, 1993.
- Foss, D. R.; Brady, J. F. *J. Rheol.* **2000**, *44*, 629.
- Russel, W.; Saville, D. A.; Schowalter, W. R. *Colloidal Dispersions*; Cambridge University Press: New York, 1992.
- Campbell, S. E.; Luengo, G.; Srdanov, V. I.; Wudl, F.; Israelachvili, J. N. *Nature (London)* **1996**, *382*, 520.
- Craig, V. S. J.; Neto, C.; Williams, D. R. M. *Phys. Rev. Lett.* **2001**, *87*, 54504.
- Baudry, J.; Charlaix, E.; Tonck, A.; Mazuyer, D. *Langmuir* **2001**, *17*, 5232.
- Zhu, Y.; Granick, S. *Phys. Rev. Lett.* **2001**, *87*, 096105.
- Thompson, P. A.; Troian, S. A. *Nature (London)* **1997**, *389*, 360.
- Thompson, P. A.; Robbins, M. O. *Phys. Rev. A* **1990**, *41*, 6830.
- Barrat, J.-L.; Bocquet, L. *Phys. Rev. Lett.* **1999**, *82*, 4671.
- Cieplak, M.; Koplick, J.; Banavar, J. R. *Phys. Rev. Lett.* **2001**, *86*, 803.
- Richardson, S. *J. Fluid Mech.* **1973**, *59*, 707.
- Jansons, K. M. *Phys. Fluids* **1998**, *31*, 15.
- Einzel, D.; Panzer, P.; Liu, M. *Phys. Rev. Lett.* **1990**, *64*, 2269.
- Zhu, Y.; Granick, S. *Phys. Rev. Lett.* **2002**, *88*, 106102.
- Russel, W.; Saville, D. A.; Schowalter, W. R. *Colloidal Dispersions*; Cambridge University Press: New York, 1992.
- Happel, J.; Brenner, H. *Low Reynolds Number Hydrodynamics*; Prentice Hall: Englewood Cliffs, NJ, 1965.
- Jabbarzadeh, A.; Atkinson, J. D.; Tanner, R. I. *Phys. Rev. E* **2000**, *61*, 690.
- Fredrickson, G. H.; Pincus, P. *Langmuir* **1991**, *7*, 786.
- Klein, J.; Kaiyama, Y.; Yoshizawa, H.; Israelachvili, J. N.; Fredrickson, G. H.; Pincus, P.; Fetters, L. J. *Macromolecules* **1993**, *26*, 5552.
- Dhinojwala, A.; Granick, S. *Macromolecules* **1997**, *30*, 1994.
- Cho, Y. K.; Dhinojwala, A.; Granick, S. *J. Polym. Sci., Polym. Phys.* **1997**, *35*, 2961.
- Israelachvili, J. N. *Pure Appl. Chem.* **1988**, *60*, 1473.
- Chan, D. Y. C.; Horn, R. G. *J. Chem. Phys.* **1985**, *83*, 5311.

- (31) Israelachvili, J. N. *J. Colloid Interface Sci.* **1985**, *110*, 263.
- (32) Georges, J. M.; Millot, S.; Loubet, J. L.; Tonck, A. *J. Chem. Phys.* **1993**, *98*, 7345.
- (33) Montfort, J. P.; Hadziioannou, G. *J. Chem. Phys.* **1988**, *88*, 7187.
- (34) Sens, P.; Marques, C. M.; Joanny, J. F. *Macromolecules* **1994**, *27*, 3812.
- (35) Stenkamp, V. S.; Berg, J. C. *Langmuir* **1997**, *13*, 3827.
- (36) Maranzano, B. J.; Wagner, N. J. *Rheol. Acta* **2000**, *39*, 483.
- (37) Israelachvili, J. N.; Kott, S. J.; Fetters, L. J. *J. Polym. Sci., Polym. Phys.* **1989**, *27*, 489.
- (38) Vinogradova, O. I. *Langmuir* **1995**, *11*, 2213.
- (39) Rushton, E.; Davies, G. A. *Int. J. Multiphase Flow* **1983**, *9*, 337.
- (40) Bechert, D. W.; Bruse, M.; Hage, W.; Meyer, R. *Naturwissenschaften* **2000**, *87*, 157.
- (41) Kataoka, D. E.; Troian, S. *Nature (London)* **1999**, *402*, 794.
- (42) Guo, P.; Weinstein, A. M.; Weinbaum, S. *Am. J. Physiol.: Renal Physiol.* **2000**, *279*, F698.

MA020043V